An Experimental and Analytical Study of the Solidification of a Binary Dendritic System

J. SZEKELY AND A. S. JASSAL

Experimental measurements are reported on the controlled solidification of a 30 pct aqueous solution of ammonium chloride in a two-dimensional slot. The actual measurements taken include the transient temperature profiles, the transient velocity fields (using tracers) and photographic observations. Through the statement of the differential energy balance and the laminar Navier-Stokes equations, written for both the liquid and the two phase regions, a mathematical model has been developed for the system. The theoretically predicted temperature and velocity profiles were found to be in good agreement with the experimentally measured values for both the two phase regions and the liquid region. For the experimental conditions the velocities in the liquid region were of the order of 0.4 to 0.8 cm/s, while the corresponding values for the two phase region were at least an order of magnitude smaller.

1. INTRODUCTION

It is an established fact that fluid flow phenomena play a major role in affecting macrosegregation during solidification processes. The interaction of fluid flow with a solidifying medium is a complex, multifaceted problem, which involves unsteady state natural convection both in the bulk of the melt and in the interdendritic region, solute redistribution due to this natural convection (macrosegregation) together with changes in the morphology due to fluid flow, *i.e.*, the shearing off of the dendrites.

The considerable practical importance of macrosegregation in affecting product quality has stimulated extensive research into this field. An elegant review of recent work in this area is available in Flemings' Howe Memorial Lecture,[1] his recent text[2] and a series of journal publications.[3-6] In this work macrosegregation was usefully represented as the effect of interdendritic flow.

Heat and fluid flow phenomena associated with (laminar) thermal natural convection in cavities have been extensively studied in recent years; rigorous mathematical representations have been developed for both steady state and unsteady state systems, which were supported by measurements.[7] These studies were extended to metallic systems by Weinberg and his coworkers.[8]

The interaction of a thermally induced convective flow field with a solidification front has also attracted both quantitative and qualitative studies.

Regarding the quantitative studies, the behavior of pure substances was investigated for both steady and unsteady conditions,[9] moreover, useful work has been done by Koump *et al*[10] in the mathematical modeling of the solidification of binary systems, albeit without taking a detailed account of the effect of thermally induced flow field.

Because of the complexity of the interaction between a thermally induced natural convective flow field and an advancing solidification front for dendrites forming in multicomponent systems, essentially qualitative studies involving transparent systems have been very helpful. In this regard, work by Hultgren and Carlson[11] with stearine melts and the more recent studies of McDonald and Hunt,[12] and Copley *et al*,[13] who used the ammonium chloride water system, are particularly noteworthy.

Finally, some comments should be made on recent work dealing with solidification in an externally imposed fluid flow field. Uhlmann *et al*,[14] Cole and Bolling,[15] and Jackson *et al*[16] have investigated the effect of externally imposed agitation (*e.g.* use of a stirrer or rotation of a mold) on the structure of the solidified structure. However, in this category the recent work of Tzavaras and Wallace[17] is perhaps the most noteworthy; these authors have shown that the dendrites may be swept away by induction stirring and that this would result in a substantially reduced inclusion count.

The brief review of earlier work may be summarized by stating that it has been demonstrated that the thermally induced flow of the melt does play a major role in macrosegregation, experienced during solidification. Various aspects of this complex problem have been investigated, but the actual interaction of thermally induced natural convection with an advancing solidification front of a binary melt has not been quantitatively studied.

The work which is described in the present paper was undertaken with the objective of providing an improved quantitative understanding of the unsteady state fluid flow phenomena that occur both in the melt and in the two-phase region during the solidification of a binary melt.

The research involved both experimental and theoretical work with emphasis on the comparison between the measurements and the predictions. In order to allow ready visual observations and velocity determination using tracers, a transparent model system has been selected for the experimental work.

Regarding the organization of the paper the apparatus, the experimental procedure and some qualitative observations will be given in Section 2, while the mathematical formulation is presented in Section 3. A comparison of the experimental measurements and the theoretical predictions is given in Section 4 and the concluding remarks are contained in Section 5.

J. SZEKELY is Professor, Department of Materials Science and Engineering, Massachusetts Institute of Technology, Cambridge, MA 02139, and A. S. JASSAL is Research Engineer, Stauffer Chemical Company, Dobbs Ferry, NY 10522.

Manuscript submitted March 12, 1976.

ISSN 0360-2141/78/0911-0389$00.75/0

2. APPARATUS AND EXPERIMENTAL PROCEDURE

2.1. The Apparatus

The objective of the experimental program was to carry out controlled solidification studies, using a binary melt, under conditions such that the visual and optical observation of the system could be complemented by both temperature measurements and by the direct estimation of the velocity fields, through the use of dye tracers. Measurements were made both under conditions when the flow field was induced by (thermal) natural convection and in the presence of an externally imposed flow field. The actual physical system employed for the study was a 30 wt pct solution of ammonium chloride in water, which was thought to be attractive, because due to its low entropy of fusion this material solidifies very much like metallic alloys. Furthermore, the transparent nature of the solution and the translucency of the ammonium chloride dendrites allow ready visual examination of the solidification process.

A schematic diagram of the apparatus is shown in Fig. 1. The apparatus consisted of a rectangular plexiglas container 40.6 cm × 6.35 cm × 15.2 cm, into which two stainless steel tanks (7.6 cm × 6.35 cm × 15.2 cm) were inserted; the inner surface of these formed the two vertical, opposing ends of the mold. The temperature of these vertical surfaces was maintained at predetermined levels by circulating fluids from thermostatically controlled reservoirs through the stainless steel cavities. In practice one of the surfaces was cooled, using methanol as a coolant, while the other surface was maintained above room temperature by circulating hot water. The apparatus was insulated using styrofoam sheets, which were removable, so as to facilitate visual and photographic observations.

The temperature within the simulated mold was monitored by twelve stainless steel sheathed copper constantan thermocouples, the output of which was recorded on a potentiometric recorder. These thermocouples were prepositioned for each run at given horizontal and vertical locations with the help of a traveling microscope.

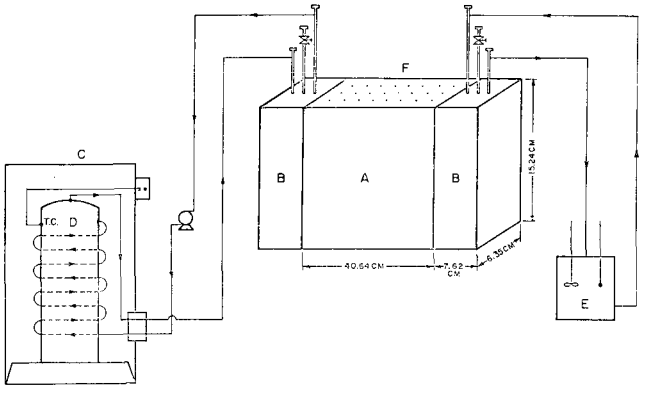

Fig. 1—Diagramatic sketch of the apparatus for natural convection study. A—Plexiglass mold, B—stainless steel tanks C—sub-zero chamber, D—coolant reservoir, E—water circulator, F—top plate for thermocouple insertion and dye injection.

An important part of the study was to obtain information on the fluid flow fields, both in the bulk of the "melt" and in the mushy zone. In the present work Schlieren photography complemented by due tracer studies, was chosen from the available techniques.[18]

A schematic layout of the Schlieren technique employed is shown in Fig. 2. It is seen that the system consisted of a light source (a mercury vapor lamp) two parabolic mirrors, a knife edge and a viewing screen. This technique relies on the fact that density changes in a transparent fluid result in changes in the refractive index, which in turn cause a deflection of the light beam. Movement of the melt, as interrelated to the density changes, could be readily observed and photographed on the screen. In the present work both still photographs and motion pictures were taken. A detailed discussion of the Schlieren technique is available in Ref. 19; here we note that this procedure is particularly attractive in the vicinity of solid surfaces, such as the dendritic region, because the measurement does not interfere with the flow field.

The actual quantitative velocity measurements were carried out with the aid of dye tracers (a methylene blue chloride solution), by timing the passage of a single streak line between two grid point marks on the front face of the plexiglas container. In using this tracer method, care was taken to ensure that both the temperature and the density of the tracer were very close to that of the melt so as to avoid any spurious external natural convection effects.

2.2. The Experimental Procedure

After assembling the apparatus and positioning of the thermocouples a 30 wt pct ammonium chloride solution was poured into the plexiglass chamber. After a few minutes when turbulence due to pouring had subsided, the coolant was pumped through a stainless steel tank, to establish a predetermined temperature at the cold face of the mold. The temperature of the hot face was also adjusted, by circulating warm water. The following measurements were made in course of a given run:

1) The temperatures were continuously recorded.

2) The advancement of the solidus and liquidus boundaries was determined visually using a Gaertner *X-Y* traveling microscope by reference to the grid marks engraved upon the front face of the plexiglas container.

3) The advancement of the solidus and liquidus fronts was also recorded photographically, using a Leica

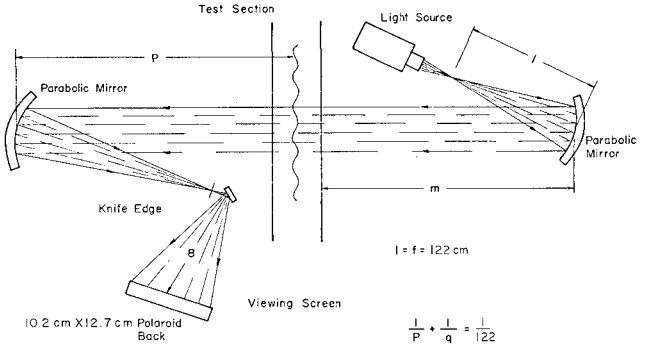

Fig. 2—Schematic diagram of the Schlieren apparatus.

camera with a close-up lens; particular attention was paid to obtaining photographs of the dendrites.

4) When the solidification front advanced to a given position within the system, dye tracer techniques were used to estimate the fluid velocities within the melt and in the interdendritic regions.

5) In order to observe the circulation patterns and in particular, the flow phenomena in the vicinity of the dendrite tips, Schlieren motion picture photographs were taken with the aid of a Bolex Camera.

2.3. Some Qualitative Observations

The qualitative measurements regarding the development of the solidification front, the temperature profiles and the velocity fields will be presented subsequently in Section 4.

However, at this stage it may be worthwhile to summarize some of the qualitative observations that were made, using still, motion picture and Schlieren photography.

These observations are summarized in the following:

i) Dendritic growth was observed in all cases, with the exception of the forced flow measurements, in which case the solid-melt interface was relatively smooth. This behavior is illustrated in Fig. 4.

ii) It was found, in agreement with the observations of previous investigators that even in case of natural convection, the flow was strong enough to shear off some of the dendrite arms, which then accumulated in the form of a debris at the bottom of the container. The fine crystals that were broken off served as "tracers" indicating the circulation of the liquid phase.

iii) The Schlieren measurements taken provided useful information on the flow field within the system without the need for external sensors or tracers. Figure 5 shows a selection of still Schlieren photographs; in these pictures the solid regions appear dark, whereas the bulk liquid shows local variations in light intensity which are due to the local variations in the refractive index. Here frames (*a*) and (*b*) show an appearance which is quite similar to "salt fingers" produced in ocean waters due to the thermohaline effect, as pointed out by Turner.[20] Frame (*c*) indicates the direction of flow in the bulk of the liquid, which is somewhat amplified by the arrows.

It is noted that a motion picture taken of the liquid movement ahead of the solidification front, which

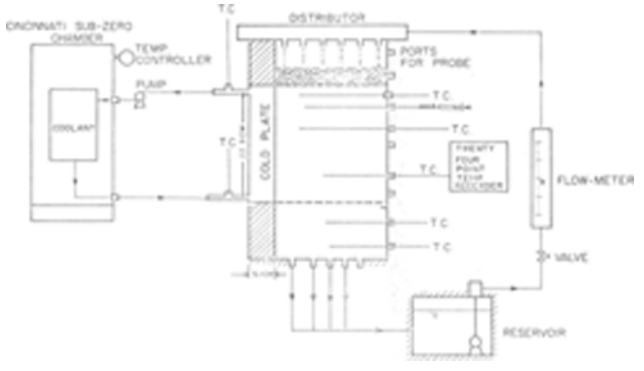

Fig. 3—Schematic diagram of the apparatus for induced flow study.

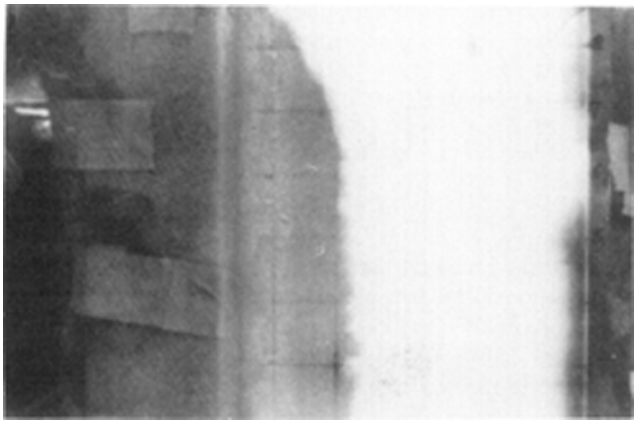

(*a*)

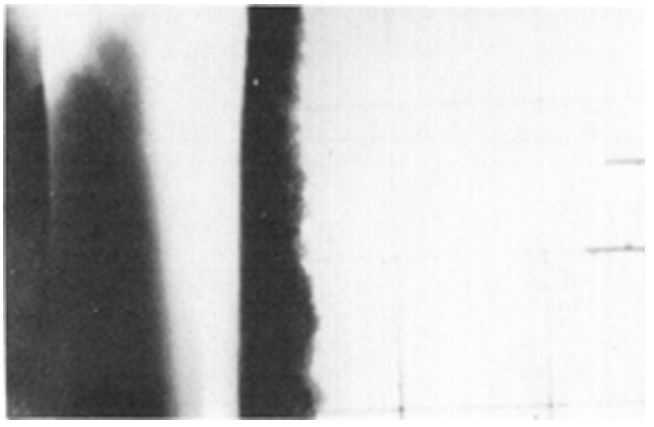

(*b*)

Fig. 4—Photograph illustrating the structure of the mushy zone, (*a*) absence of forced flow, and (*b*) after inducing flow through the system. Notice the smooth structure in (*b*).

cannot be reproduced here, provides a rather better indication of the dynamic nature of the flow field even in the vicinity of the dendritic region.

However, the Schlieren technique was found to be particularly helpful for recording the jet like eruptions of liquid (partially denuded of ammonium chloride), rejected by the advancing solidification front, as illustrated in Fig. 6 which shows ascending liquid entities which tend to rise because of their lower ammonium chloride content and hence lower density.

3. FORMULATION

In order to develop a quantitative representation of the transient development of the temperature and fluid flow fields within the system let us consider the solidification of a binary melt, placed in a rectangular container, extending from $x = 0$ to $x = W$ and from $y = 0$ to $y = L$ and which is large in the z direction. Initially the whole space is occupied by molten material at a uniform temperature $T_{m,i}$. Then at time = 0 the plane corresponding to $x = 0$ is suddenly brought to a temperature T_c, which is well below the eutectic temperature T_E, while the surface corresponding to the $x = W$ plane is maintained at a temperature T_W, which is well above the liquidus. At the same time the surfaces corresponding to the $y = 0$ and $y = L$ planes are insulated.

As a result natural convection currents will be set up in the molten region. Moreover, a solidification

front will form and experience growth in the x direction. More specifically, two regions may be identified, namely a completely solidified zone (below the eutectic temperature in the present case) and a two phase or "mushy" region within the temperature range $T_E \leq T \leq T_L$ where the solid and liquid phases coexist, albeit the fraction of solid is a function of the actual temperature. This system is sketched in Fig. 7.

The objective of the formulation to be developed here is to obtain expressions for the temperature distribution within the system, together with the description of the (transient) velocity fields both in the molten and in the two phase regions. In order to allow the statement of the problem in a mathematically manageable form, the following simplifying assumptions will be made:

1) Except for the effect of the density difference in driving the natural convective flow, the physical properties of the molten and the solid phases are assumed to be constant.

2) The density of the liquid in the two phase (mushy) zone is assumed to depend on the temperature and on the fraction of solids.

3) The entrained crystallites in the liquid are assumed to have no effect on the physical properties.

Within the framework of these assumptions the problem may be stated by writing the unsteady state thermal energy balance for the solid, mushy and the liquid

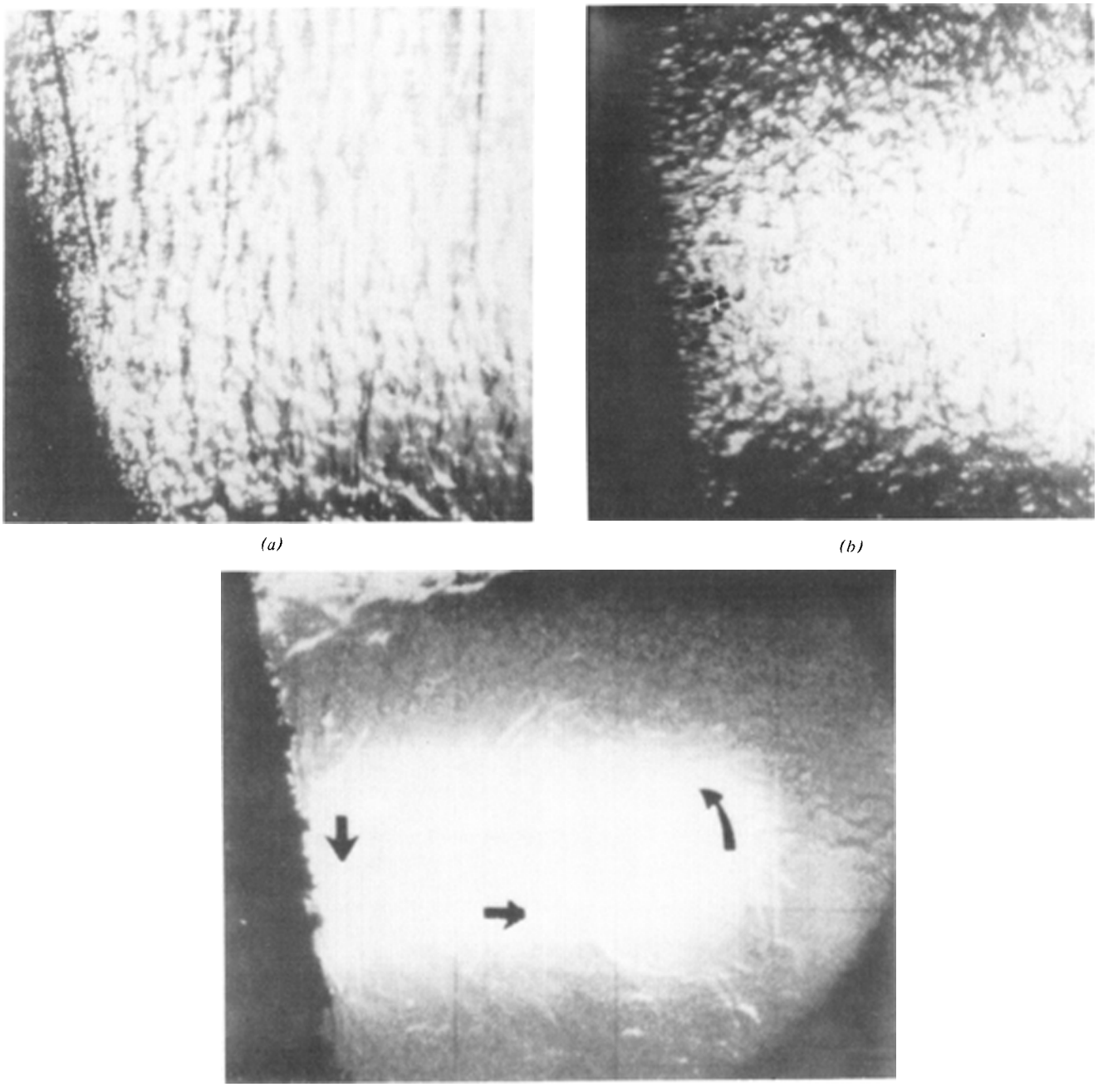

Fig. 5—Schlieren photographs ahead of the solidification front showing the flow patterns in the bulk liquid as a result of natural convection; (*a*) and (*b*) indicate density variations, magnification 115 times.

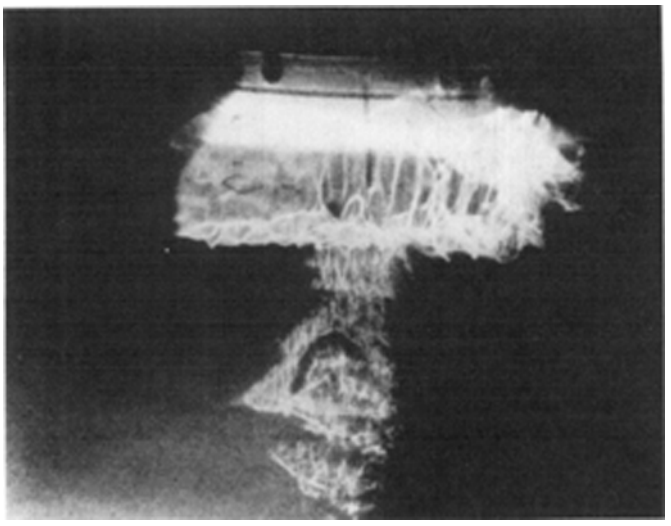

Fig. 6—Photograph reproduced from the Schlieren movie showing the jets ascending opposite to the direction of gravity ahead of the mushy zone. Magnification 0.82 times.

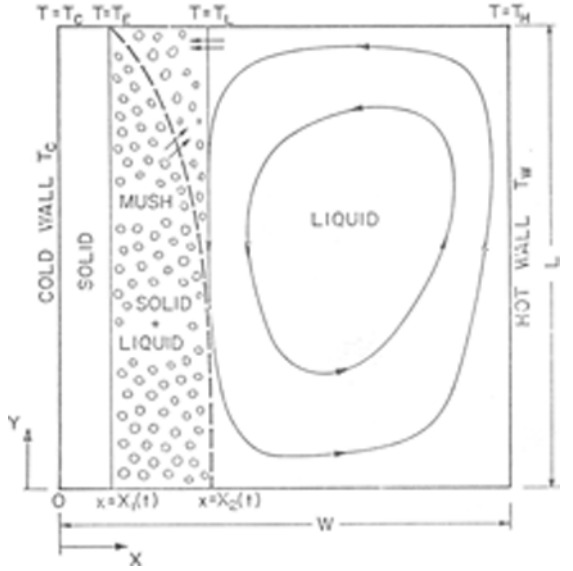

Fig. 7—Schematic representation of the coordinate system indicating the thermal boundary conditions.

regions, together with the appropriate forms of the equation of motion.

ENERGY BALANCES

Thus we have energy balance in the solid region:

$$\frac{\partial T_s}{\partial t} = \alpha_s \left(\frac{\partial^2 T_s}{\partial x^2} + \frac{\partial^2 T_s}{\partial y^2} \right); \quad \begin{matrix} 0 \le x \le X_1(t) \\ 0 \le y \le L \end{matrix} \quad [1]$$

Energy balance in the two phase region:

$$(C_p\rho)_m \frac{\partial T_m}{\partial t} + (C_p\rho)\, l \left(u_{x,m} \frac{\partial T_m}{\partial x} + u_{y,m} \frac{\partial T_m}{\partial y} \right)$$

$$= k_m \left(\frac{\partial^2 T_m}{\partial x^2} + \frac{\partial^2 T_m}{\partial y^2} \right) + A \quad [2]$$

$$X_1(t) \le x \le X_2(t) \qquad 0 \le y \le L$$

where,

$$A = \rho_m \Delta H \left(\frac{\partial f_s}{\partial T_m} \cdot \frac{\partial T_m}{\partial t} \right) \quad [3]$$

represents the rate of heat generation in the two phase region due to solidification.

$$\rho_m = \rho_S f_S + \rho_L (1 - f_S);$$

is the density of the two phase region. f_S is the fraction of solids, while the subscripts m, and l refer to the solid, two phase and the liquid regions respectively.

Energy balance in the liquid region

$$\frac{\partial T_l}{\partial t} + u_x \frac{\partial T_l}{\partial x} + u_y \frac{\partial T_l}{\partial_y} = \alpha_l \left[\frac{\partial^2 T_l}{\partial x^2} + \frac{\partial^2 T_l}{\partial y^2} \right] \quad [4]$$

$$X_2(t) \le x \le W$$

$$0 \le y \le L .$$

Fluid Flow Equations

The two components of the equation of motion in the two-phase region may be written as:

$$\frac{\partial u_{x,m}}{\partial t} + u_{x,m} \frac{\partial u_{x,m}}{\partial x} + u_{y,m} \frac{\partial u_{x,m}}{\partial y} = -\frac{1}{\rho_m} \frac{\partial p}{\partial x} - \frac{\nu}{K_p} u_{x,m} \quad [5]$$

and

$$X_1(t) \le x \le X_2(t)$$

$$\frac{\partial u_{y,m}}{\partial t} + u_x \frac{\partial u_{y,m}}{\partial \chi} + u_y \frac{\partial u_{y,m}}{\partial y} = -\frac{1}{\rho_m} \frac{\partial p}{\partial y} - \frac{\nu}{K_p} u_{y,m} - g \quad [6]$$

$$X_1(t) \le x \le X_2(t).$$

Here g is the acceleration due to gravity acting in the y direction.

In writing Eqs. [5] and [6] the interdendritic region was regarded as a porous medium and thus the viscous terms in the Navier-Stokes equations were replaced by the resistance terms in Darcy's equation; here K_p, the permeability of the medium, was considered a function of f_S, the fraction of solids.

According to accepted convention in the field of natural convection heat transfer, the pressure terms appearing in Eqs. [5] and [6] were considered to account for the sum of the static pressure and the incremental pressure change due to density variation and fluid motion.

The two components of the equation of motion in the liquid region may be written as:

$$\frac{\partial u_{x,l}}{\partial t} + u_{x,l} \frac{\partial u_{x,l}}{\partial x} + u_{y,L} \frac{\partial u_{x,l}}{\partial_y} = -\frac{1}{\rho_l} \frac{\partial P}{\partial x}$$

$$+ \nu \left[\frac{\partial^2 u_{x,l}}{\partial x^2} + \frac{\partial^2 u_{x,l}}{\partial y^2} \right]; \; X_2(t) \le x \le W \quad [7]$$

$$\frac{\partial u_{y,l}}{\partial t} + u_{x,l} \frac{\partial u_{y,l}}{\partial x} + u_{y,l} \frac{\partial u_{y,l}}{\partial y} = -\frac{1}{\rho_l} \frac{\partial P}{\partial y} - g$$

$$+ \nu \left[\frac{\partial^2 u_{y,l}}{\partial x^2} + \frac{\partial^2 u_{y,l}}{\partial y^2} \right] ; X_2(t) \leq x \leq W. \qquad [8]$$

Finally the equation of continuity may be expressed as:

$$\frac{\partial u_{x,m}}{\partial x} + \frac{\partial u_{y,m}}{\partial y} = 0 \qquad [9]$$

(for the two-phase region)

$$\frac{\partial u_{x,l}}{\partial x} + \frac{\partial u_{y,l}}{\partial y} = 0 \qquad [10]$$

(for the liquid region).

Equations [1] through [10] express the conservation of thermal energy, the momentum balance and the conservation of matter (continuity) in the system.

The statement of the problem may now be completed by writing down the boundary conditions and by specifying certain functional relationships between the process variables in the two-phase zone.

Boundary Conditions

The boundary conditions have to express the following constraints imposed on the system.

Boundary Conditions on Temperature. 1) The temperature is specified at the surfaces corresponding to $x = 0$ and $x = W$, 2) initially the whole system is molten and at a constant temperature, 3) the surfaces corresponding to $y = 0$ and $y = L$ are insulated, and 4) the temperature and the heat flux are continuous across the $X_1(t)$ and the $X_2(t)$ planes.

We note here that because of the way in which the heat balance equations were written, the release of the latent heat occurs in the two-phase zone (see Eqs. [2] and [3]). It follows that the characteristic moving boundary type boundary conditions did not have to be invoked, rather the position of the liquidus and solidus lines, $X_1(t)$ and $X_2(t)$ is defined implicitly by:

$$T_m = T_S = T_E \text{ at } x = X_1(t) \qquad [11]$$

and

$$T_m = T_L \text{ at } x = X_2(t). \qquad [12]$$

The Boundary Conditions on Velocity. The boundary conditions on velocity have to express the following: 5) both velocity components are zero at all the solid bounding surfaces, *i.e.*, at $y = 0$, at $y = L$, at $x = X_1(t)$ and at $x = W$, 6) the velocity is a continuous function of distance at the boundary between the liquidus front and the bulk fluid, *i.e.* at $x = X_2(t)$, and 7) the initial velocity within the fluid is zero. The mathematical expression of the boundary conditions is not reproduced here, but is available in the thesis upon which this paper is based.[26]

Subsidiary Relationships

The principal subsidiary relationships needed are the relationship between the fraction of solids in the two-phase region and the temperature together with an equation for K_p, the permeability of the porous medium which appeared in Eqs. [5] and [6]. The following expression was derived from the phase diagram:

$$f_s = 1 - \frac{\bar{k}}{1 - \bar{k}} \left[\frac{1}{\bar{k}} - \frac{m_L C_0}{T - T^*} \right] \qquad [13]$$

where,

f_s is the fraction of solids,

$\bar{k}$ is the equilibrium distribution coefficient which varies with composition of liquid ($C_E \leq C_l \leq C_0$),

m_L is the slope of the liquidus line,

C_0 is the initial composition of the NH_4Cl-H_2O solution,

C_E is the eutectic composition,

T^* is the temperature represented by the intercept of the liquidus line on the temperature axis, and

K_p is the permeability of the interdendritic region was approximated by the following expression (Ref. [21]):

$$K_p = \frac{(1 - f_s)\,\bar{\delta}^2}{32} \qquad [14]$$

where $\bar{\delta}$ the average dendrite arm spacing was estimated as around 100 μ.

Equations [1] through [14] together with the associated boundary conditions provide a complete definition of the problem.

Before proceeding with the numerical solution of this system of equations, it is convenient and customary to recast the fluid flow equations in terms of the vorticity and the stream function. For a two-dimensional system in cartesian coordinates these quantities are defined as follows:

$$\xi = \frac{\partial u_y}{\partial x} - \frac{\partial u_x}{\partial y} \qquad [15]$$

(vorticity)

$$u_x = \frac{\partial \psi}{\partial y}; \; u_y = -\frac{\partial \psi}{\partial x} \qquad [16] \text{ and } [17]$$

(stream function).

Moreover, ξ and ψ are related by:

$$\xi = -\left[\frac{\partial^2 \psi}{\partial x^2} + \frac{\partial^2 \psi}{\partial y^2} \right]. \qquad [18]$$

These definitions are valid for both the two-phase and for the liquid regions.

Through the use of the stream function the equation of continuity is automatically satisfied, furthermore, the vorticity enables one to combine the two components of the equation of motion in a single expression.

Thus, after some standard manipulation[22] Eqs. [5] and [6] may be written as:

$$\frac{\partial \xi_m}{\partial t} + u_{x,m} \frac{\partial \xi}{\partial x} + u_{y,m} \frac{\partial \xi}{\partial y} = g_x \beta \frac{\partial T_m}{\partial x} - \frac{\nu}{K_p} \xi \qquad [19]$$

where β is the coefficient of thermal expansion.*

*A full discussion of the steps involved in transforming Eqs. [5] and [6] to Eq. [10] is available in Refs. 22 and 23.

The equivalent expression of Eqs. [7] and [8] is given as:

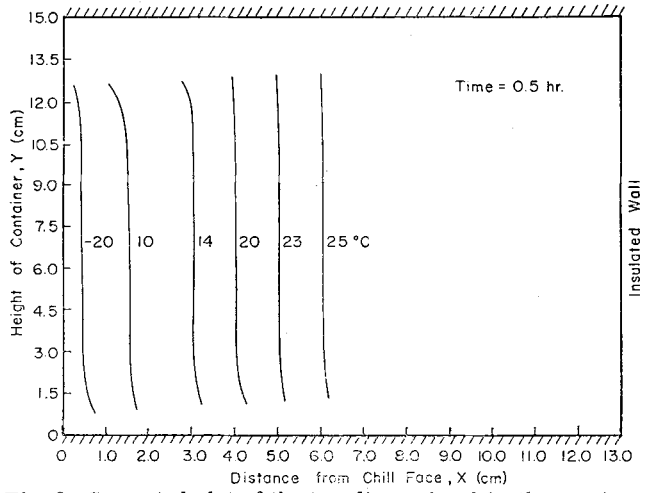

Fig. 8—Computed plot of the two dimensional isotherms in the system at 0.5 h.

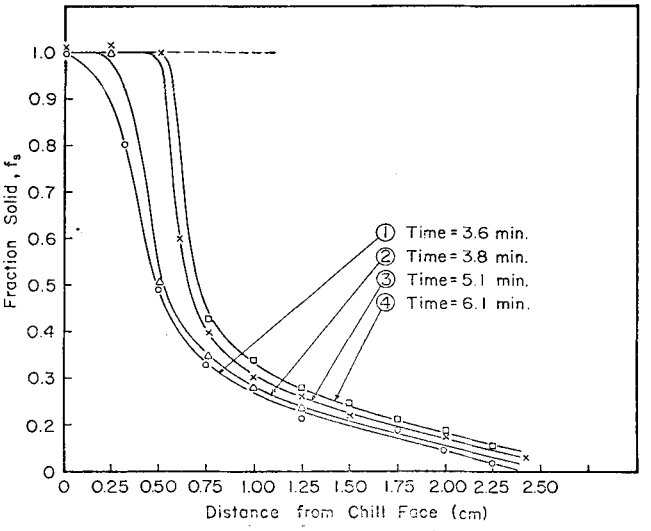

Fig. 9—Computed curves of fraction solid as a function of distance from chill face at various times and at a height of 10 cm in the system.

$$\frac{\partial \xi_l}{\partial t} + u_{x,l}\frac{\partial \xi}{\partial x} + u_{y,l}\frac{\partial \xi}{\partial y} = g_x\beta\frac{\partial T_l}{\partial x} + \nu\left[\frac{\partial^2 \xi}{\partial x^2} + \frac{\partial^2 \xi}{\partial y^2}\right]. \qquad [20]$$

The governing Eqs. [1], [2], [4], [18], [19] and [20] were put in a finite difference form and were solved numerically. An 11 × 11 grid was employed for each, the two-phase, the liquid and the solid region; the alternating direction implicit method[23,24] was used for solving the parabolic Eqs. [2], [4], [19], [20] while the technique of successive over-relaxation[25] was used for integrating the elliptic Eq. [18].

The CDC 6400 digital computer of the State University of New York at Buffalo was used and the total computer time requirement was of the order of 60 seconds per run. The property values used in the computation are summarized in Section 6. The complete listing of the computer program is available in Ref. 26.

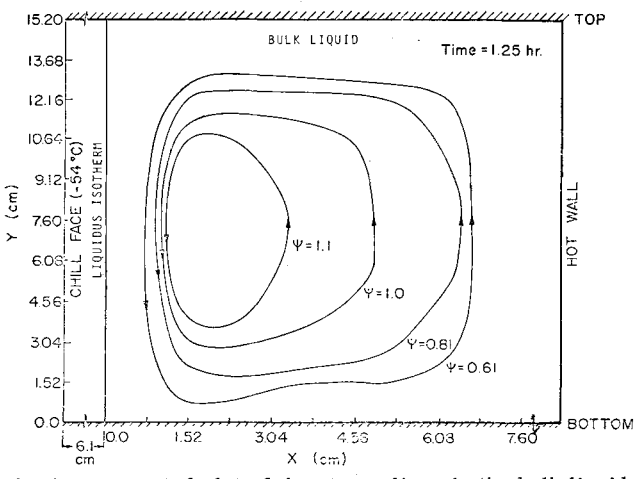

Fig. 10—Computed plot of the streamlines in the bulk liquid at 1.25 h.

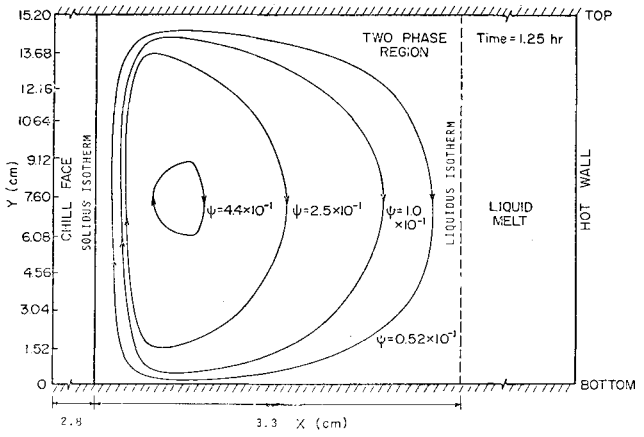

Fig. 11—Computed plot of the streamlines in the mushy zone at 1.25 h.

4. RESULTS

The following figures (8 to 11) show a selection of the computed results depicting the development of the temperature profiles solidus and liquidus fronts and the circulation patterns in the system.

Figure 8 shows the computed isotherms after an interval of 30 min. The steep temperature gradients in the solid, the relatively uniform temperature fields in the bulk of the melt and the existence of a thermal boundary layer in the vicinity of the liquidus isotherm are all readily discernible from this graph.

Figure 9 shows an example plot of the computed solid fraction profiles as a function of the distance from the chill face, at a constant vertical height of 10 cm from the bottom with time as a parameter; the substantial width of the two-phase zone is readily seen in this graph.

Figures 10 and 11 show the computed streamline patterns, which indicate the direction of the circulation; it is of interest to note that the absolute velocities appear to be much larger in the bulk liquid than in the two-phase region, moreover, the circulation pattern in the two-phase region seems to be profoundly influenced by the flow field in the melt. Of much greater interest, however, is to compare the predic-

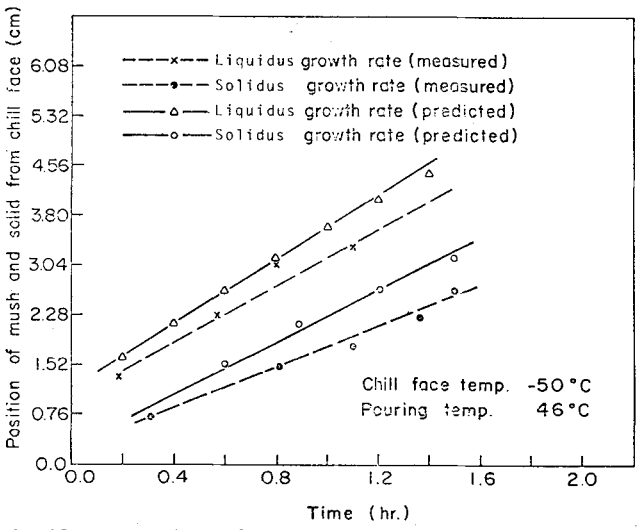

Fig. 12—Comparison of the computed and measured growth of the solidus and liquidus boundaries at a height of 4.0 in. in the system.

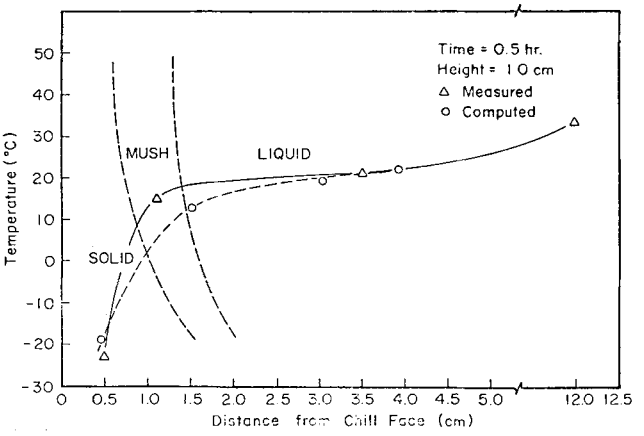

Fig. 13—Plot of the measured temperature distribution in the system at 0.5 h and at a height of 10.0 cm in the container.

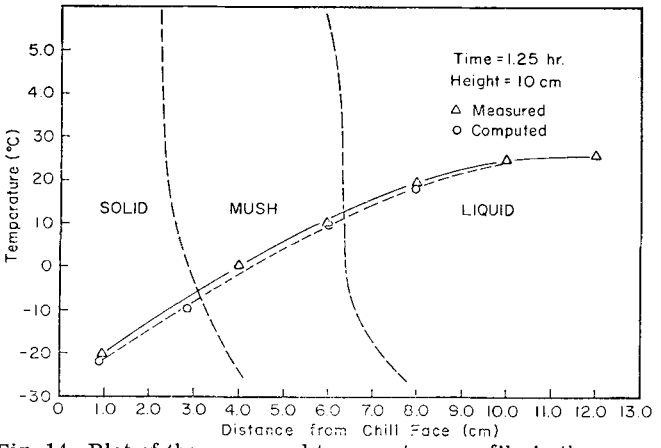

Fig. 14—Plot of the measured temperature profile in the system at 12.5 h.

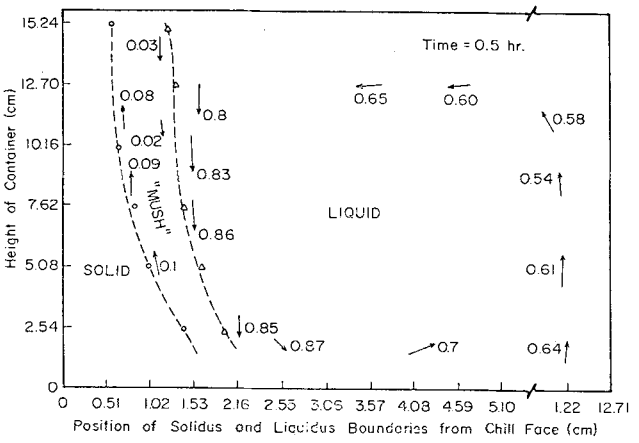

Fig. 15—Velocity distribution in the mushy zone and in the bulk liquid at 0.5 h (measured, cm/s).

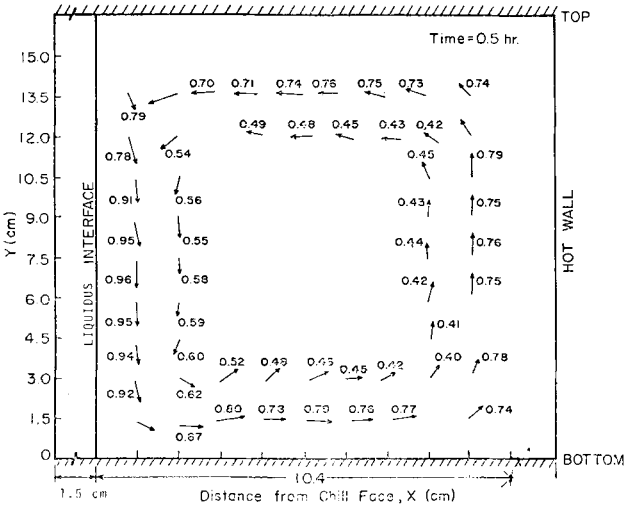

Fig. 16—Computed plot of the magnitude of the velocity field in the bulk liquid at 0.5 h.

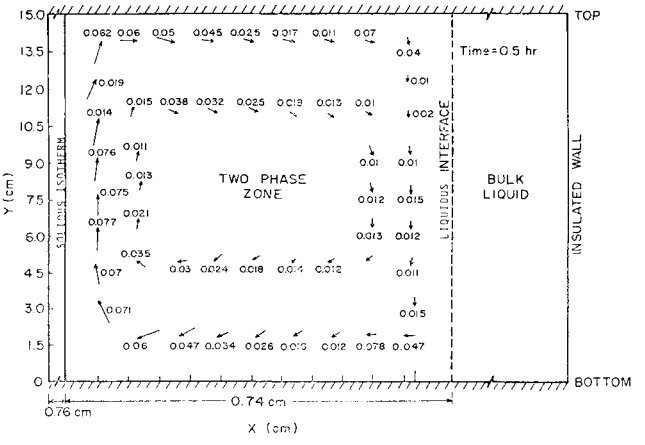

Fig. 17—Computed plot of the magnitude of the velocity field (cm/s) in the mushy zone at 0.5 h.

tions made on the basis of the analysis with actual measurements. This is done in the following Figs. 12 to 20.

Figure 12 shows a comparison between the measured and the predicted positions of the solidus and the liquidus fronts, as a function of time at a height of some 10 cm from the bottom of the container, where the effect of erosion or debris deposition are thought to be the least significant. The agreement between measurements and predictions is thought to be reasonable; however, this is not a very critical test of the model because the advancement of the solidus and

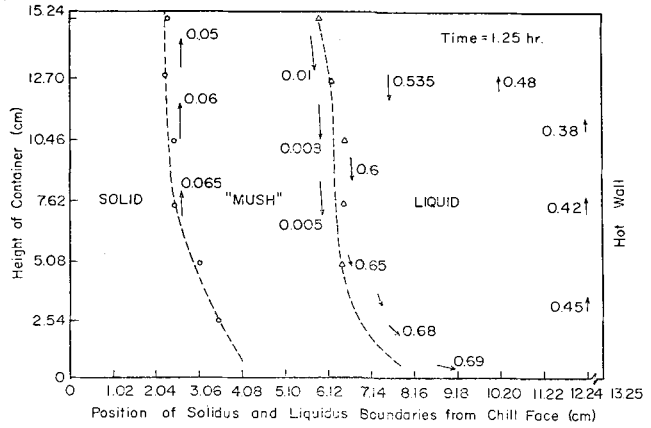

Fig. 18—Velocity distribution in the mushy zone and in the bulk liquid at 1.25 h (measured cm/s).

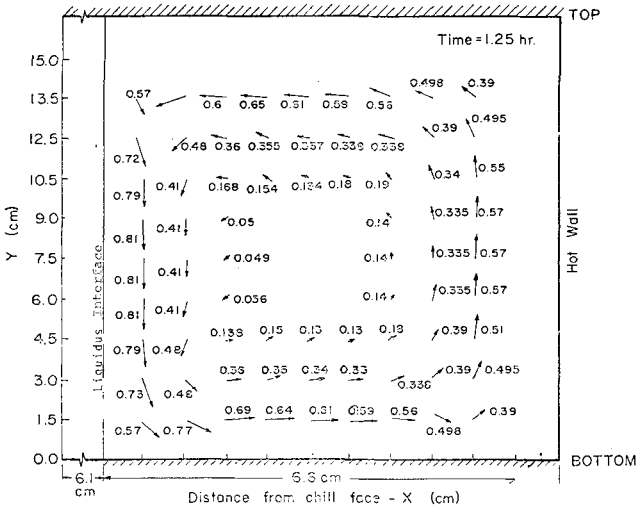

Fig. 19—Computed plot of the magnitude of the velocity field (cm/s) in the bulk liquid at 1.25 h.

liquidus fronts is probably controlled largely by conduction rather than the convection phenomena.

Figure 13 shows a comparison between the measured and the predicted temperature profiles after a time of 30 min at a height of 10 cm. Figure 14 shows a comparison between the measured and the predicted temperature profiles after a time of 75 min and here the agreement is very good indeed.

One of the principal objectives of the investigation was to develop predictive expressions for the velocity fields in both the bulk liquid and in the two-phase zone, and to compare these predictions with measurements.

Figure 15 shows a plot of the experimentally determined values of the velocity field in both the two-phase and in the liquid regions after a lapsed time of 30 min. The corresponding computed values of the velocity field in the bulk liquid and in the two-phase zones are given in Figs. 16 and 17 respectively. It is seen that the agreement between measurements and predictions is quite good both with regard to the qualitative nature of the circulation patterns and the absolute magnitudes of the velocity vector.

Figure 18 shows the measured map of the velocity vectors after a time lapse of 75 min, while the corresponding predictions are given in Figs. 19 and 20

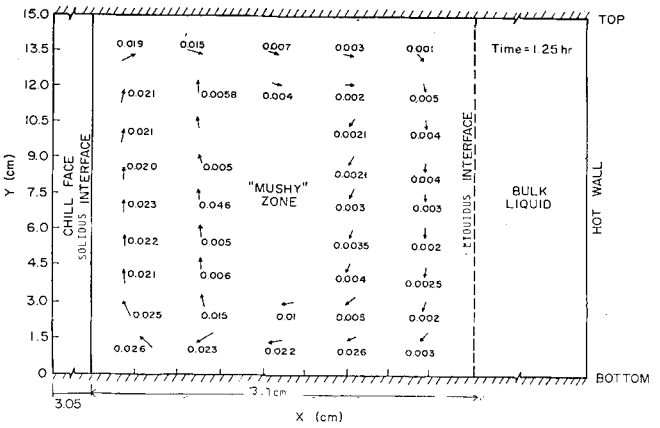

Fig. 20—Computed plot of the magnitude of the velocity field (cm/s) in the mushy zone at 1.25 h.

for the bulk liquid and the two-phase zone respectively. The agreement is again quite reasonable; moreover, both predictions and measurements are consistent in giving lower absolute values for the circulation rates.

The discrepancy between the measured and the predicted values of the velocity vector in the two-phase zone seems greater in this case, but this may be attributable to the increased experimental uncertainty involved in measuring the very low velocities.

5. CONCLUDING REMARKS

Experimental measurements were made of the transient development of the temperature and the fluid flow fields in the controlled solidification of a 30 pct ammonium chloride-water mixture. Furthermore, a mathematical representation was developed for describing the unsteady state temperature and velocity fields in the controlled solidification of an ammonium chloride water mixture in a rectangular cavity.

The statement of the problem involved the establishment of differential thermal energy balances in the solid, "two phase" and in the liquid regions together with the appropriate equations of motion for both the two phase and the liquid zones. The qualitative observations made, through the use of Schlieren photography regarding the shearing off of the dendrite arms and the jetlike eruption of the interdendritic fluid were in general agreement with the findings of previous investigators. The resultant, simultaneous, partial differential equations were solved numerically using a digital computer.

The theoretically predicted temperature profiles and velocity fields in the bulk liquid and in the two phase region were found to be in reasonably good agreement with measurements. An important finding of interest was the fact that for the experimental conditions the velocity field in the bulk liquid had a marked effect on the velocity field established in the two phase region. It is suggested that the modeling of solidification processes through the combined statement of the equations of motion (in the melt and in the two phase zone) and the energy balance equation is a sound and feasible approach which should provide an improved insight into the microscopic behavior of the system. The fol-

lowing qualifying observations should be made, however:

1) If the sole purpose of modeling were to predict the solidification rates, the problem would be greatly simplified because fluid flow is unlikely to play a major role in affecting the rate of solidification.

2) While the mathematical representation developed here was able to predict reasonably accurately both the solidification rates and the velocity fields, the modeling of other important facets of the problem, such as the erosion of dendrites, instabilities resulting in jetlike fluid emissions from the two-phase zone and intensive local circulation rates in the interdendritic spaces would require much greater mathematical sophistication.

3) The natural convection driven fluid flow phenomena in ingot solidification are likely to be rather more complex than the somewhat idealized system examined in this work. These additional complexities would be attributable to the fact that the flow field would be turbulent (because of the larger physical size) moreover, the circulation in the bulk melt would be much more strongly time dependent than in the case examined here.

It is thought, nonetheless that the quantitative approach developed in this paper, which is supported by experimental measurements, should provide a first step toward the tackling of these much more complex problems, usefully augmenting earlier work by Weinberg[27,28] and Szekely.[29]

6. PHYSICAL CONSTANTS USED

k_l = thermal conductivity of liquid phase = 0.468 W/m K,
k_s = thermal conductivity of solid phase = 0.393 W/m K,
ρ_s = density of solid phase = 1102 kg/m^3,
ρ_l = density of liquid solution = 1013 kg/m^3,
T_{so} = temperature of solidus (eutectic) = 257.4 K,
T_{li} = initial temperature of melt (solution) = 313.2 K,
$C_{\rho s}$ = specific heat of solid = 1.87 KJ/kg K,
$C_{\rho l}$ = specific heat of liquid = 3.249 KJ/kg K,
ΔH = latent heat of fusion or crystallization 313.8 KJ/kg,
μ_l = viscosity of liquid = 1.3×10^{-3} kg/ms,
β = temperature coefficient of cubical expansion = (18.6×10^{-5})/K,
$\overline{k}$ = equilibrium distribution coefficient $\simeq$ 3.333,
m_L = slope of the liquidus line = 8.6 K/(wt pct NH_4Cl),
C = initial concentration of solution (melt) = 30 wt pct NH_4Cl, and
T^* = temperature represented by the intercept of the liquidus line on the temperature axis = 222.8 K.

NOMENCLATURE

Symbol	Definition
C_0	= initial concentration of the melt,
C_p	= specific heat of the liquid,
g	= gravitational constant,
f_s	= fraction solidified,
ΔH	= latent heat of fusion of crystallization,
k	= thermal conductivity,
L	= height of container,
m_L	= slope of the liquidus line on the phase diagram,
P	= pressure,
t	= time,
T	= temperature,
T_i	= initial temperature of the melt,
T_{so}	= solidus temperature of system,
T_E	= eutectic temperature of system,
T_{Li}	= liquidus temperature of system,
u_x	= velocity of the fluid in the x direction,
u_y	= velocity of the fluid in the y direction,
$X_1(t)$	= reference position of the solidus boundary from chill face, and
$X_2(t)$	= reference position of the liquidus boundary from the chill face.

Greek Symbols	Definition
$\alpha = \frac{k}{\rho c_p}$	= thermal diffusivity,
β	= temperature coefficient of cubical expansion,
ξ	= vorticity,
μ	= viscosity,
ν	= kinematic viscosity,
ρ	= density, and
ψ	= stream function.

Subscripts m, l and s refer to the two-phase, liquid and solid regions respectively.

REFERENCES

1. M. C. Flemings: "1974 Howe Memorial Lecture of the Iron and Steel Division," *Met. Trans.*, 1974, vol. 5, pp. 2121-34.
2. M. C. Flemings: *Solidification Processing*, McGraw Hill, N.Y., 1974.
3. M. C. Flemings, R. Mehrabian, and G. E. Nereo: *Trans. TMS-AIME*, 1968, vol. 242, pp. 41-49.
4. T. S. Piwonka and M. C. Flemings: *Trans. TMS-AIME*, 1968, vol. 236, p. 1157.
5. R. Mehrabian and M. C. Flemings: *Trans. TMS-AIME*, 1969, vol. 245, p. 2349.
6. *Ibid, Met. Trans.*, 1970, vol. 1, pp. 1209-20.
7. J. Szekely and M. R. Todd: *Int. Heat and Mass Transfer*, 1971, vol. 14, pp. 467-82.
8. M. J. Stewart and F. Weinberg: *Met. Trans.*, 1972, vol. 3, pp. 333-37.
9. J. Szekely and P. S. Chabbra: *Met. Trans.*, 1970, vol. 1, p. 1195.
10. V. Koump and R. H. Tien: *Trans. ASME*, 1970, vol. 12, pp. 11-16.
11. A. Hultgren and C. G. Carlson: *Jernkont. Ann.*, 1936, vol. 120, pp. 600-15.
12. R. J. McDonald and J. S. Hunt: *Trans. TMS-AIME*, 1969, vol. 245, pp. 1993-99.
13. S. M. Copley, A. F. Giamei, S. M. Johnson, and M. F. Hornbecker: *Met. Trans.*, 1970, vol. 1, p. 2193.
14. D. Uhlmann, T. Seward, and B. Chalmers: *Trans. TMS-AIME*, 1966, vol. 236, p. 527.
15. G. S. Cole and G. F. Bolling: *Trans. TMS-AIME*, 1965, vol. 233, pp. 1568-72.
16. K. A. Jackson: "Dendritic Solidification," Movie, Bell Labs.
17. A. A. Tzavaras and J. F. Wallace: *J. of Crys. Growth*, 1971, p. 782.
18. Flow Visualization Symposium, ASME, New York, 1960.
19. "Physical Measurements in Gas Dynamics and Combustion" R. W. Ladenburg, ed., Princeton University Press, New York, 1964.
20. J. S. Turner: *Deep Sea Res.*, 1967, vol. 14, pp. 599-611.
21. A. E. Scheidegger: *The Physics of Flow Through Porous Media*, p. 116, Macmillan Press, New York, 1960.
22. J. O. Wilkes and S. W. Churchill: *AIChE J.*, 1966, vol. 12, pp. 161-66.
23. M. R. Todd: Ph.D. Thesis, State University of New York at Buffalo, 1969.
24. J. Douglas, Jr. and J. W. Gunn: *Num. Math.*, 1964, vol. 6, p. 428.
25. M. Clark and K. F. Hanse: *Numerical Methods of Reactor Analysis*, pp. 125-29, Academic Press, New York, 1964.
26. A. S. Jassal: Ph.D. Thesis, State University of New York at Buffalo, 1975.
27. M. J. Stewart and F. Weinberg: *Met. Trans.*, 1972, vol. 3, pp. 333-36.
28. L. C. MacAuley and F. Weinberg: *Met. Trans.*, 1973, vol. 4, pp. 2097-2107.
29. J. Szekely and J. H. Chen: in *Chemical Metallurgy of Iron and Steel*, p. 218, The Iron and Steel Institute, 1971.